ACS OMEGA

http://pubs.acs.org/journal/acsodf

Article

Efficient Extraction of Olefin from Liquid-Phase Olefin/Alkane Mixtures Using Novel Bimetallic Ionic Liquids

Jiaxin Cui, Mengfan Yin, Tao Zheng, Han Liu, Rui Zhang,* Haiyan Liu, Zhichang Liu, Chunming Xu, and Xianghai Meng*

Cite This: *ACS Omega* 2025, 10, 17744−17757

Read Online

ACCESS | Metrics & More | Article Recommendations | Supporting Information

ABSTRACT: The separation of olefins and alkanes is beneficial for resource utilization of oil products, and liquid−liquid extraction is an important method of liquid-phase olefin/alkane separation. This study investigated the feasibility of bimetallic ionic liquids for the extraction of olefin from liquid-phase olefin/alkane mixtures using 1-hexene/*n*-hexane as a model hydrocarbon mixture. The bimetallic ionic liquids were first synthesized from different metal chlorides ($ZnCl_2$, $SnCl_2$, $AlCl_3$, $FeCl_3$) and CuCl with triethylamine hydrochloride. This newly prepared Fe−Cu bimetallic ionic liquid $[Et_3NH]Cl-0.47FeCl_3$-0.8CuCl had a good extraction performance, and the extraction selectivity could reach up to 8.41, which was about 4 times that of the organic solvent such as *N*-formylmorpholine and *γ*-butyrolactone used in the industry. The liquid−liquid equilibrium (LLE) of 1-hexene/*n*-hexane and Fe−Cu bimetallic ionic liquid system was investigated under different extraction temperatures, extraction times, and mass ratios of extractant to feed. Through 5 recycling experiments, the extraction selectivity decreased by less than 2%, and the characteristic peaks of the recovered bimetallic ionic liquids were unchanged by IR analysis, which proved that the bimetallic ionic liquid had excellent reversibility. Furthermore, the mechanism of 1-hexene extraction was investigated by quantum chemistry calculation and Raman spectroscopy, and there was *π*-complexation between Cu^+ and 1-hexene. Then, the charge density of Cu^+ in bimetallic ionic liquids was larger than that of cuprous-based ionic liquids. The results revealed that the addition of $FeCl_3$ could activate Cu^+ and weaken the Cu−Cl bond, enhancing the ability of the bimetallic ionic liquid to extract 1-hexene. Therefore, $[Et_3NH]Cl-0.47FeCl_3$-0.8CuCl was a good potential extractant during the efficient extraction of 1-hexene.

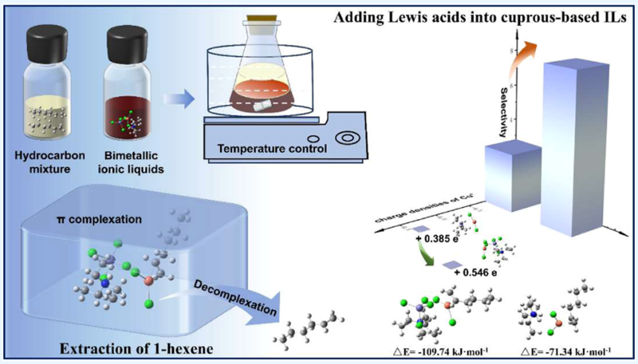

1. INTRODUCTION

Achieving green and low-carbon development of the petrochemical industry requires efficient utilization of petroleum resources. The development of efficient separation techniques is conducive to increasing the value of petroleum. The separation of olefins/alkanes has been a main energy-intensive and high-cost process in the petrochemical industry. Olefin and alkane molecules with the same carbon number have molecular similarities.[1,2] Since the differences in boiling point, relative volatility, and molecular size are small, it is difficult to separate olefins/alkanes without requiring substantial energy input.[3,4] The separation process of gaseous olefins/alkanes is relatively mature at present, but the separation of liquid-phase olefins/alkanes has been less researched. As an important chemical feedstock, liquid-phase olefins have been widely used as a copolymerization monomer for the production of polymers and in the synthesis of halogenated hydrocarbons.[5] In the process of producing liquid-phase olefin, it has been found that liquid-phase olefin is mostly mixed with alkanes.[6,7] Thus, the separation of liquid-phase olefin/alkane mixtures economically and efficiently is challenging work.

Conventional separation processes, such as distillation, suffer from high energy consumption and many separation stages.[8,9] In recent years, facilitated transport membranes have been extensively researched and applied to separate olefin/alkane mixtures, especially membranes containing the Ag^+ and Cu^+ complex olefins.[10,11] However, facilitated transport membranes are difficult for large-scale applications because of limited transportation capacity and high production expenses.[12] Liquid−liquid extraction has the advantages of simple processes, and the energy consumption was lower than distillation.[13] It is expected to be a favorable means for

Received: January 8, 2025
Revised: April 3, 2025
Accepted: April 11, 2025
Published: April 25, 2025

https://doi.org/10.1021/acsomega.5c00224

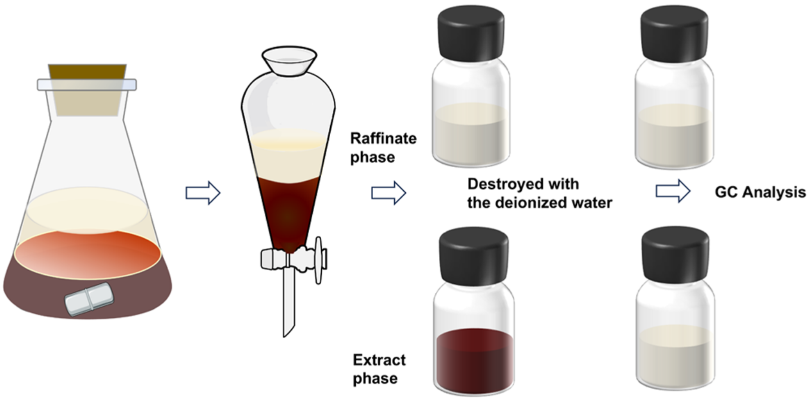

Figure 1. Extraction equilibrium experiments.

olefin/alkane separation. The extractant is crucial to efficient extraction.[14] Traditional organic solvents such as *N*-formylmorpholine (NFM) and *γ*-butyrolactone (GBL) were used as extractants. The selectivity of 1-hexene was around 2 and had volatilization loss.[15] Efficient extractants could be developed to overcome the defects of traditional organic extractants in the extraction of olefin.

Ionic liquids (ILs) can be ideal extractants with both ionic and organic properties, less likely to contaminate olefins in subsequent separations and easy to recover.[16,17] Previous studies have focused on the selective separation of olefin/alkane using ionic liquids (ILs) containing transition metals.[18] The direct addition of silver salts to ionic liquids is simple and has received much attention. Mortaheb et al.[19] introduced $Ag[NO_3]$ into $[Bmim][NO_3]$ for the separation of ethene/ethane, having 5 times the absolute absorptivity of ethene than pure ILs. Ortiz et al.[20] investigated the influence of the anions structure of imidazole ILs with silver salts to separate propene/propane and found that $[BF_4]^-$ anion had better selectivity than $[Tf_2N]^-$ and $[NO_3]^-$ anions. Wu et al.[21] synthesized protic imidazole ionic liquids with silver salts, which had a high ethene separation selectivity, indicating that protic imidazole ILs with silver salts had excellent application prospects.

Extractants containing silver salts show excellent selectivity for olefin separation, but the high price is a drawback. Reducing the cost of extractants is a vital factor in industrial applications. Economically, cuprous ions are more advantageous than silver ions. Yu et al.[22,23] prepared Cu^+-ILs, such as [Emim][Br]-CuBr, [Bmim][Br]-CuBr, [Emim][SCN]-CuSCN, and [Bmim][SCN]-CuSCN, had excellent separation selectivity (11.8−13.9) for propene and had good reusability. To further improve the separation effect, the development of bimetallic ionic liquids is a worthy direction to explore. Although bimetallic ionic liquids are less studied in the field of separation, they are widely used in catalysis,[24] analysis,[25] and absorption[26] due to the unique synergistic effect of the two metal anions. Inspired by synergistic mechanisms, novel bimetallic ionic liquid extractants could be synthesized to separate liquid-phase olefin/alkane mixtures by screening metals and optimizing the molar ratio of the two metals. There is a specific reversible interaction between Cu^+ and the olefin. Cuprous chloride (CuCl) is a common and inexpensive metal salt. Some Lewis acids with suitable acidity[27] can interact with CuCl and are expected to enhance the ability of Cu^+ to complex with olefins.[28] Bimetallic ionic liquids were designed based on the specific interaction of Cu^+ with olefins, and the synergistic enhancement of Lewis acids is expected to achieve efficient extraction of olefins.

In this study, novel bimetallic ionic liquids containing different metal chlorides (MCly; M = Zn, Sn, Al, or Fe) and CuCl were used as extractants for the separation of liquid-phase olefin/alkane mixtures. Due to the separation mechanism being consistent and 1-hexene being a high commercial value product in the petrochemical industry, 1-hexene/*n*-hexane was used as a model mixture to explore the extraction strategy of liquid-phase olefin by bimetallic ionic liquids. The effects of the metal chloride species, concentration, and bimetallic ionic liquid cation structure were investigated. The effects of extraction temperature, extraction time, and mass ratio of extractant to feed on separation performance were investigated by liquid−liquid phase equilibrium experiments. The cyclic stability of bimetallic ionic liquids was evaluated via recycling experiments. Furthermore, Raman spectroscopy analysis and quantum chemistry calculations were employed to reveal the separation mechanism of bimetallic ionic liquid with 1-hexene and *n*-hexane.

2. EXPERIMENT

2.1. Experimental Materials. Cuprous chloride (CuCl) (≥98%), ferric chloride ($FeCl_3$) (≥98%), aluminum chloride ($AlCl_3$) (≥98%), stannous chloride ($SnCl_2$) (≥98%), zinc chloride (≥98%), 1-hexene (1-C_6H_{12}) (≥99%), *n*-hexane (*n*-C_6H_{14}) (≥99%), *n*-heptane (*n*-C_7H_{16}) (≥99%), *n*-dodecane (*n*-$C_{12}H_{26}$) (≥99%), and 1-butyl-3-methylimidazolium chloride ([Bmim]Cl) (≥98%) were purchased from Beijing InnoChem Science & Technology Co., Ltd. Triethylamine hydrochloride ($[Et_3NH]Cl$) (≥98%) and *N*-butyl-3-methylpyridine chloride ([Bmpy]Cl) (≥98%) were purchased from Shanghai Aladdin Biochemical Technology Co., Ltd.

2.2. Preparation of Ionic Liquids. Single metal ionic liquids: taking $[Et_3NH]Cl$-nCuCl for example: $[Et_3NH]Cl$-nCuCl was synthesized by stirring the $[Et_3NH]Cl$ and the required molar ratio of CuCl powders at 120 °C for 4 h under nitrogen protection.

Bimetallic ionic liquids: taking [Cation]Cl-m$FeCl_3$-nCuCl for example: [Cation]Cl-m$FeCl_3$-nCuCl was synthesized through two steps. First, the [Cation]Cl and a certain amount of $FeCl_3$ powders were stirred at 120 °C for 2 h under nitrogen protection to obtain [Cation]Cl-m$FeCl_3$. Then, the required molar ratio of CuCl powder was stirred with the [Cation]Cl-m$FeCl_3$ at 150 °C for 4 h under nitrogen protection. The synthesized ionic liquids (Figures S1 and S2) were stored in a glovebox for later use.

2.3. Extraction Equilibrium Experiments. The mixture of 1-hexene and *n*-hexane with a mass ratio of 1:1 was selected as the model oil. The model oil (5 g) was added to the conical flask (30 mL), and then, a certain mass of IL was also added to this conical flask. The mixture was stirred with a magneton at a stirring speed of 1200 rpm for a certain extraction time to ensure extraction equilibrium and controlled at a certain extraction temperature with a uniform speed programmed temperature control tank.

The extract phase and raffinate phase were separated by the funnel. The upper and lower samples were successively pretreated to avoid contamination of the chromatographic column by the ionic liquid. The samples were destroyed with deionized water and diluted with *n*-heptane or *n*-dodecane. Pretreatment method: sample (3 g) and deionized water (100 g) were added to a conical flask (250 mL) and stirred for 0.5 h until the ionic liquid was destroyed. Then, *n*-heptane or *n*-dodecane (3 g) was mixed in the system and stirred for 0.3 h. Phase separation was also carried out through the funnel. The sample of the oil phase (upper layer) was taken for the gas chromatography (GC) analysis (Figure 1). To exclude the influence of deionized water treatment on the tested components, liquid−liquid equilibrium was performed on reference samples such as deionized water + 1-hexene + *n*-hexane, deionized water + triethylamine hydrochloride + 1-hexene + *n*-hexane, and deionized water + bimetallic ionic liquid + 1-hexene + *n*-hexane. The results are listed in Table 1. The effect of pretreatment on the relative composition of the hydrocarbons was negligible, and deionized water did not affect the results.

Table 1. Influence of Pretreatment on the Extraction Results

samples	condition	$x_{1\text{-hexene}}$	$x_{n\text{-hexane}}$
1-hexene + *n*-hexane		0.5006	0.4994
1-hexene + *n*-hexane	deionized water treatment	0.5010	0.4990
triethylamine hydrochloride + 1-hexene + *n*-hexane	deionized water treatment	0.5007	0.4993
bimetallic ionic liquid + 1-hexene + *n*-hexane (upper layer)		0.4655	0.5345
bimetallic ionic liquid + 1-hexene + *n*-hexane (upper layer)	deionized water treatment	0.4652	0.5348

2.4. Analytical Methods. The composition of the oil phase sample was characterized by a 3420A gas chromatograph with a flame ionization detector (FID) and an HB-PONA column. For the ionic liquid sample, the structure was analyzed by a Fourier transform infrared (FT-IR) spectrometer (Bruker TENSOR-27), including a spectral range of 400−4000 cm^{-1}. The LabRAM Odyssey Raman spectrometer was used to analyze the interaction mechanism of Fe−Cu bimetallic ionic liquid with 1-hexene and *n*-hexane. The surface chemistry was analyzed by X-ray photoelectron spectroscopy (XPS) using a Thermo Scientific ESCALAB 250Xi. Thermogravimetric analysis (TGA) was performed using a Rigaku TG-DAT 8122 system with the sample exposed to flowing nitrogen gas. The metal contents were analyzed by an inductively coupled plasma-optical emission spectrometer (ICP-OES) of PerkinElmer. Viscosity was measured by an Ubbelohde viscometer, and density was measured by an SY-1 densitometer.

2.5. Extraction Evaluation Indexes. To quantitatively characterize the extraction performance of the extractant, the following indexes (distribution coefficient (*D*), extraction selectivity (*S*), and extraction performance index (*PI*)) are defined as follows.

$$D_i = \frac{x_i^{\text{E}}}{x_i^{\text{R}}} \tag{1}$$

$$S_{1\text{-hexene}} = \frac{D_{1\text{-hexene}}}{D_{n\text{-hexane}}} \tag{2}$$

$$\text{PI} = D_{1\text{-hexene}} \times S_{1\text{-hexene}} \tag{3}$$

where x_i is the mass fraction of component *i*, while E and R represent the extract phases and raffinate phases, respectively.

2.6. Experimental Repeatability Verification. The repeatability experiments of olefin extraction were verified to determine the reliability of the experimental process and method. The reliability of the extraction experiment was verified by taking bimetallic ionic liquid $[\text{Et}_3\text{NH}]\text{Cl}-0.47\text{FeCl}_3-0.8\text{CuCl}$ as an extractant. The liquid−liquid equilibrium experiments were investigated with pressure, extraction temperature, extraction time, mass ratio of 1-hexene to *n*-hexane, and mass ratio of extractant to feed, keeping constant at 1 atm, 10 °C, 2 h, 1:1, and 2:1. The extraction experiment was repeated three times. The results are listed in Table S1. For each index, the population standard deviation and the relative mean deviation were also relatively small, among which the relative mean deviation of the olefin extraction performance index was the largest (1.7%). The above results indicated that the extraction experiment had good repeatability and reliable data.

2.7. Computation Details. Gaussian 09[29] was used to optimize the structure under PBE0[30]/ma-def2-svp[31] with the dispersion correction with Becke and Johnson damping (D3BJ).[32] The Natural bond orbital (NBO) method analyzed the charge of Cu^+. The energy calculations were carried out at a higher level of PWPB95-D3(BJ)[33]/ma-def2qzvpp.[31] The basis set superposition error (BSSE) needs to be considered for the calculation of the interaction energy between the two substances.[34] The interaction energy calculated using counterpoise correction in ORCA software[35] was the energy obtained after considering the BSSE correction. Multiwfn[36] and VMD[37] software were used to carry out wave function analysis and visualization of the analysis, respectively.

3. RESULTS AND DISCUSSIONS

3.1. Structural Design of Ionic Liquid Extractants.

3.1.1. Effect of Different Coordination Metal Species and Concentrations. The effect of coordination metal species and concentrations in the ionic liquid on the extraction was investigated. The extraction pressure, extraction temperature, extraction time, mass ratio of 1-hexene to *n*-hexane, and mass ratio of extractant to feed were 1 atm, 30 °C, 2 h, 1:1, and 2:1, respectively. The high melting point (53 ± 1 °C) of $[\text{Et}_3\text{NH}]\text{Cl}-0.5\text{ZnCl}_2-1.0\text{CuCl}$ caused the extractant to be solid at 30 °C. The extraction experiment with $[\text{Et}_3\text{NH}]\text{Cl}-0.5\text{ZnCl}_2-1.0\text{CuCl}$ as an extractant was carried out at 55 °C. (The higher extraction temperatures could cause larger energy consumption in the extraction; therefore, $[\text{Et}_3\text{NH}]\text{Cl}-$

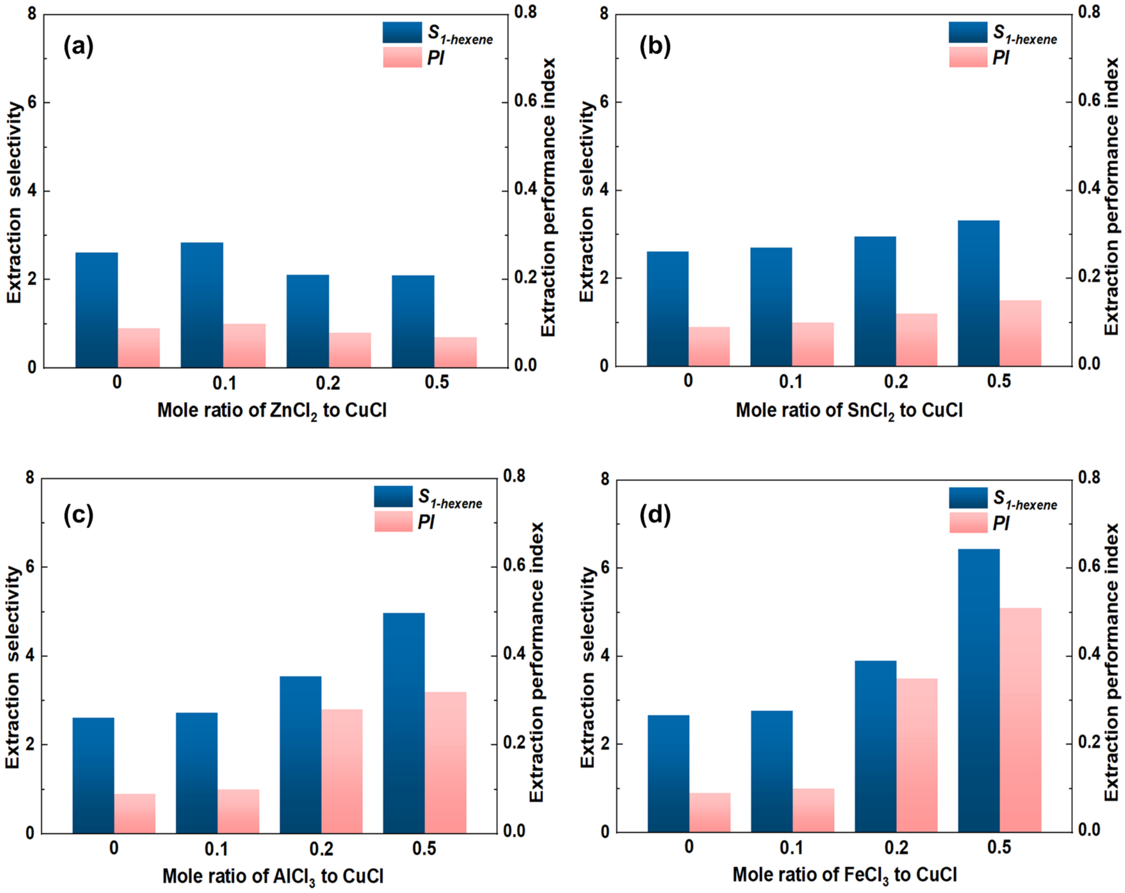

Figure 2. Effect of mole ratio of (a) $ZnCl_2$ to CuCl, (b) $SnCl_2$ to CuCl, (c) $AlCl_3$ to CuCl, and (d) $FeCl_3$ to CuCl on the extraction selectivity and the extraction performance index.

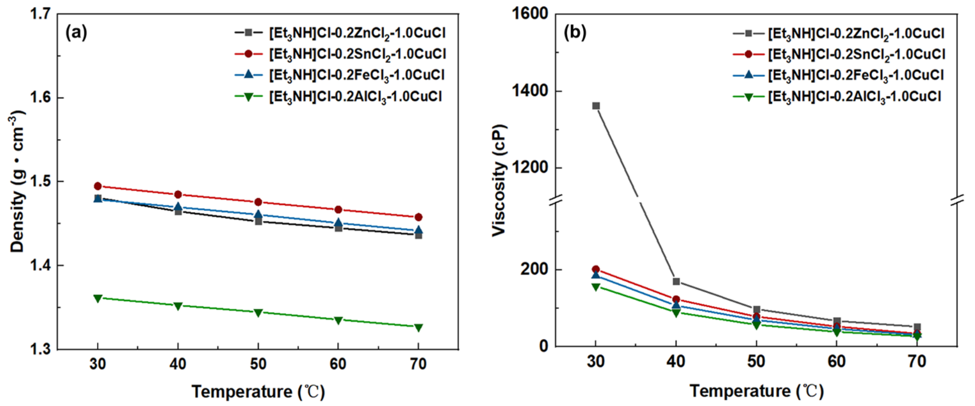

Figure 3. (a) Densities and (b) viscosities of bimetallic ionic liquid.

$0.5ZnCl_2$−1.0CuCl was not suitable as an extractant for the separation of 1-hexene/*n*-hexane.)

Figure 2 indicated that the extraction effect of ionic liquid increased, followed by a decrease with the addition of $ZnCl_2$. For the Al−Cu, Fe−Cu, and Sn−Cu bimetallic ionic liquid, the extraction selectivity and the extraction performance index increased with the increasing concentration of metal halides. The growth trend was more pronounced for Fe−Cu bimetallic ionic liquid. The extraction selectivity of $[Et_3NH]Cl$−$0.5FeCl_3$−1.0CuCl for 1-hexene was 6.68, which was about 3 times that of $[Et_3NH]Cl$−1.0CuCl. Fe−Cu bimetallic ionic liquid showed more advantages in separating 1-hexene/*n*-hexane.

The extraction effect of the Zn−Cu bimetallic ionic liquid was different from that of other bimetallic ionic liquids, which might be due to changes in viscosity. The viscosity and density data of the extractant are the basic physical properties required to perform liquid−liquid extraction. As shown in Figure 3, when the mole ratio of first metal chlorides to CuCl was 0.2, the sequence of viscosity was as follows: $[Et_3NH]Cl$−$0.2ZnCl_2$−1.0CuCl > $[Et_3NH]Cl$−$0.2SnCl_2$−1.0CuCl > $[Et_3NH]Cl$−$0.2FeCl_3$−1.0CuCl > $[Et_3NH]Cl$−$0.2AlCl_3$−1.0CuCl. The Zn−Cu bimetallic ionic liquid changed from

Table 2. Separation Performance of 1-Hexene/*n*-Hexane Using Fe−Cu Bimetallic Ionic Liquids and Mixed Extractants

extractant	$S_{\text{1-hexene}}$	$D_{\text{1-hexene}}$	PI
$[Et_3NH]Cl-0.4FeCl_3-0.9CuCl$	7.01	0.070	0.49
$[Et_3NH]Cl-0.43FeCl_3-0.85CuCl$	6.85	0.076	0.52
$[Et_3NH]Cl-0.47FeCl_3-0.8CuCl$	6.69	0.079	0.53
$[Et_3NH]Cl-0.5FeCl_3-0.75CuCl$	5.80	0.079	0.46
$[Et_3NH]Cl-0.94FeCl_3$ + $[Et_3NH]Cl-1.6CuCl$	5.52	0.078	0.43

solid to liquid near 30 °C and had the problem of high viscosity (1362.5 cP). It was unfavorable for mass transfer and limited olefin extraction. The density difference between the bimetallic ionic liquid and the mixed hydrocarbon was moderate, which was conducive to phase separation. Then, the density and viscosity for bimetallic ionic liquid were fitted by eqs 4 and 5,[38] respectively (Tables S2−S5, S7, and S8).

$$\rho = a + bT \tag{4}$$

$$\eta = \eta_0 e^{-E_a/RT} \tag{5}$$

3.1.2. Effect of the Molar Ratio of $FeCl_3$ to CuCl. Although $[Et_3NH]Cl-0.5FeCl_3-1.0CuCl$ had a good separation performance, it had obvious solid precipitation, and it was necessary to search for the optimal bimetallic content and ratio. The actual metal content of $[Et_3NH]Cl-0.5FeCl_3-1.0CuCl$ was about 85% of the theoretical value determined by ICP-OES. Bimetallic ionic liquids $[Et_3NH]Cl-0.4FeCl_3-0.9CuCl$, $[Et_3NH]Cl-0.43FeCl_3-0.85CuCl$, $[Et_3NH]Cl-0.47FeCl_3-0.8CuCl$, and $[Et_3NH]Cl-0.5FeCl_3-0.75CuCl$ were synthesized experimentally. As shown in Table 2, a slight increase in the molar ratio of $FeCl_3$ to CuCl would improve the olefin solubility in bimetallic ionic liquids but would lead to a decrease in the extraction selectivity of olefin, such as $[Et_3NH]Cl-0.4FeCl_3-0.9CuCl$ had higher extraction selectivity, but its solubility to 1-hexene was relatively lower than that of $[Et_3NH]Cl-0.47FeCl_3-0.8CuCl$. $[Et_3NH]Cl-0.47FeCl_3-0.8CuCl$ had a high extraction selectivity (6.69) and was favorable for dissolving 1-hexene. Therefore, it had the highest extraction performance index (0.53) among the four synthesized bimetallic ionic liquids, which was a good extractant for separating 1-hexene/*n*-hexane.

In addition, $[Et_3NH]Cl-0.94FeCl_3$ and $[Et_3NH]Cl-1.6CuCl$ mixture (mass ratio of 1:1) as a mixed extractant for 1-hexene/*n*-hexane separation under the same conditions was investigated. (The mixed extractant had the same composition as $[Et_3NH]Cl-0.47FeCl_3-0.8CuCl$). For mixed extractants, the extraction selectivity was 5.52, and the extraction performance index was 0.43, which were lower than those of $[Et_3NH]Cl-0.47FeCl_3-0.8CuCl$. This indicated that bimetallic ionic liquids were different from the physical mixing of the two metallic ionic liquids. The interaction of two metal ions affected the ability of bimetallic IL to extract olefin. 1-Hexene could interact with Cu^+ by π-bond complexation, and electron transfer of two metal ions could improve the activity of Cu^+. The synergistic action of two metal ions in the Fe−Cu bimetallic ionic liquid enhanced the extraction effect of 1-hexene.

3.1.3. Effect of Fe−Cu Bimetallic IL Cation Structure. Evaluation of the effect of Fe−Cu bimetallic IL cation structure on 1-hexene/*n*-hexane separation was performed. Different cationic donors ($[Et_3NH]Cl$, [Bmim]Cl, and [Bmpy]Cl) were selected to synthesize bimetallic ILs. The LLE experiments were investigated with pressure, extraction temperature, extraction time, mass ratio of 1-hexene to *n*-hexane, and mass ratio of extractant to feed, keeping constant at 1 atm, 30 °C, 2 h, 1:1, and 2:1. Table 3 showed the ionic liquid with $[Et_3NH]^+$ as the cation had the highest extraction selectivity and extraction performance index, while the cost was relatively lower than those of the other two ionic liquids. Therefore, $[Et_3NH]Cl-0.47FeCl_3-0.8CuCl$ was selected for subsequent studies.

Table 3. Effect of Cations on the Extraction Effect of Bimetallic Ionic Liquids

bimetallic ionic liquid	$S_{\text{1-hexene}}$	$D_{\text{1-hexene}}$	PI
$[Et_3NH]Cl-0.47FeCl_3-0.8CuCl$	6.69	0.079	0.53
$[Bmim]Cl-0.47FeCl_3-0.8CuCl$	5.31	0.061	0.32
$[Bmpy]Cl-0.47FeCl_3-0.8CuCl$	4.33	0.060	0.26

3.2. Characterization of Bimetallic Ionic Liquid.

3.2.1. XPS Analysis of Fe−Cu Bimetallic Ionic Liquids. The bimetallic ionic liquid $[Et_3NH]Cl-0.47FeCl_3-0.8CuCl$ was analyzed by XPS. As depicted in Figure 4, XPS revealed the presence of C, Cl, N, Cu, Fe, and O (XPS test exposure to air caused). The nature of the copper species in the bimetallic ionic liquid could be determined by the Cu 2p spectral regions. Cuprous ions were unstable under conventional conditions, leading to a weakening of the complexation effect, so it was necessary to consider the form of copper ions present in bimetallic ionic liquids. It might be observed that the Cu $2p_{3/2}$ peak at a binding energy, E_b, of 932.4 eV,[39] which was likely to be Cu(I), being present in the form of CuCl (E_b = 932.5 eV).[39] It revealed that Cu^+ could be stabilized in Fe−Cu bimetallic ionic liquid. XPS revealed a Fe $2p_{3/2}$ peak and a Fe $2p_{1/2}$ peak at a binding energy, E_b, of 711.4 and 724.7 eV. In addition, there was a satellite peak near 718.8 eV. The above results confirmed the presence of Fe^{3+} species on IL surfaces.[40]

3.2.2. Thermal Stability of Fe−Cu Bimetallic Ionic Liquids. The thermal stability of the extractant is important in industrial applications. TGA was applied to analyze the thermal properties of the Fe−Cu bimetallic ionic liquid $[Et_3NH]Cl-0.47FeCl_3-0.8CuCl$. The TG and DTG curves in the range of 30−600 °C are shown in Figure 5. The bimetallic ionic liquid had a weight loss of 61.8% from 230 to 473 °C. The peak temperature of the DTG curve corresponded to the temperature at which the weight loss of Fe−Cu bimetallic ionic liquid was rapid. Fe−Cu bimetallic ionic liquid had strong weight losses around 330 and 390 °C. The results indicated that weight losses occurred in both anions and cations. In particular, the sublimation temperature of triethylamine hydrochloride was lower than that of metal chloride, so the weight losses of cations were earlier than that of anions.

The thermal decomposition temperature of the bimetallic ionic liquid was over 230 °C. It was higher than that of organic solvents commonly used in the industry such as *N*-formylmorpholine and γ-butyrolactone (<150 °C), indicating

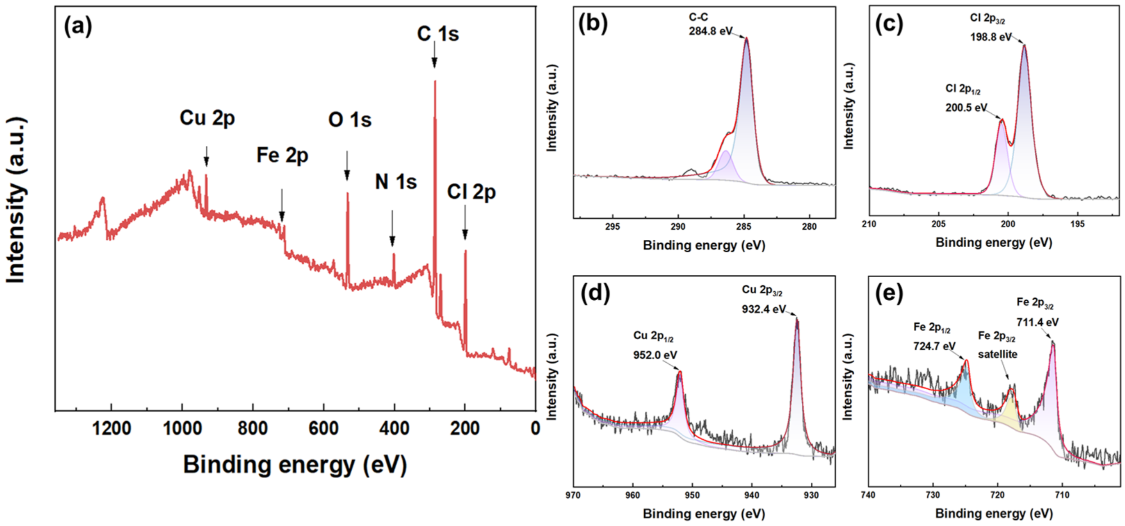

Figure 4. XPS spectra of Fe−Cu bimetallic ionic liquid: (a) survey scan; (b) C 1s; (c) Cl 2p; (d) Cu 2p; and (e) Fe 2p.

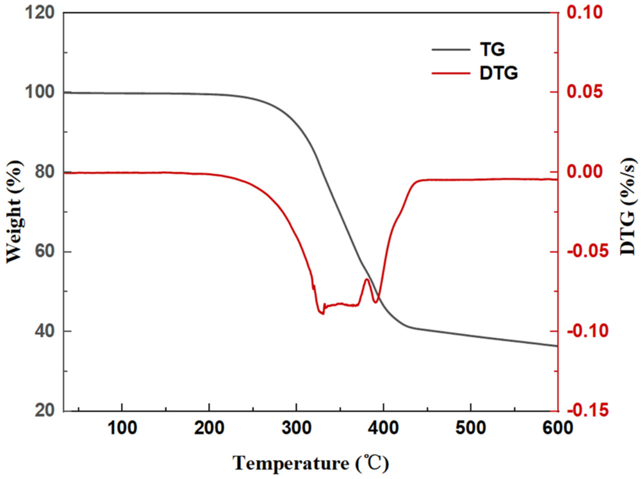

Figure 5. TG and DTG curves of the Fe−Cu bimetallic ionic liquid.

that bimetallic ionic liquid had more advantages in the olefin/alkane separation. In addition, the separation of liquid-phase olefin/alkane mixtures, especially the fractions of C8−C10, required a recycling temperature of about 200 °C. The thermal decomposition temperature of the bimetallic ionic liquid was above 230 °C, which indicated that it had thermal stability when recycling liquid-phase olefins from other fractions.

3.3. Optimization of Liquid−Liquid Extraction Conditions.

3.3.1. Effect of Extraction Temperature. The effect of the extraction temperature on separation was investigated. The extraction pressure, extraction time, mass ratio of 1-hexene to *n*-hexane, and mass ratio of extractant to feed were 1 atm, 2 h, 1:1, and 2:1, respectively. Figure 6 shows that with the increase of extraction temperature, the distribution coefficient of 1-hexene decreased, and the distribution coefficient of *n*-hexane increased. As a result, the extraction selectivity and extraction performance of 1-hexene gradually decreased. The extraction selectivity was 8.41, and the extraction performance index was 0.71 at the extraction temperature of 10 °C. The effect of temperature on extraction was significant. The increase of temperature reduced the viscosity of the Fe−Cu bimetallic ionic liquid, facilitated the movement and collision between ionic liquid and mixed hydrocarbon, and increased the molecular diffusion rate. It was beneficial to dissolve the mixed hydrocarbon in an Fe−Cu bimetallic ionic liquid. Physical dissolution mainly depended on weak interactions, such as the van der Waals force or hydrogen bond between molecules. The contribution to the extraction process was relatively small and usually appeared as

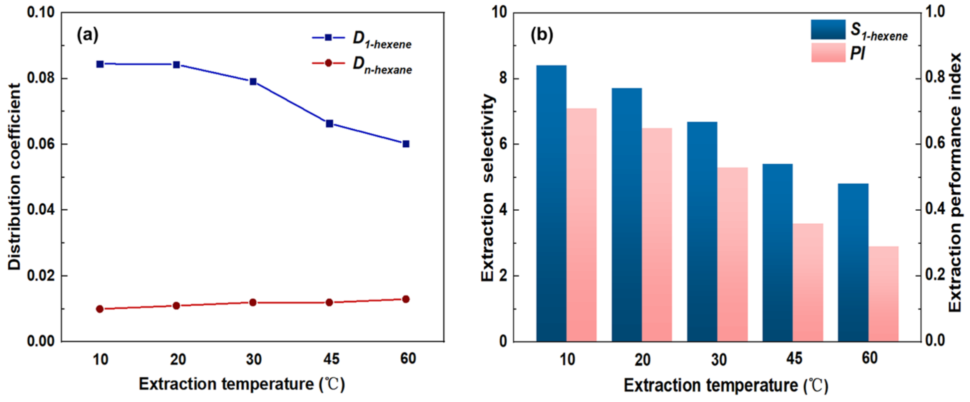

Figure 6. Influence of extraction temperature on (a) the distribution coefficient, (b) the extraction selectivity, and the extraction performance index of 1-hexene.

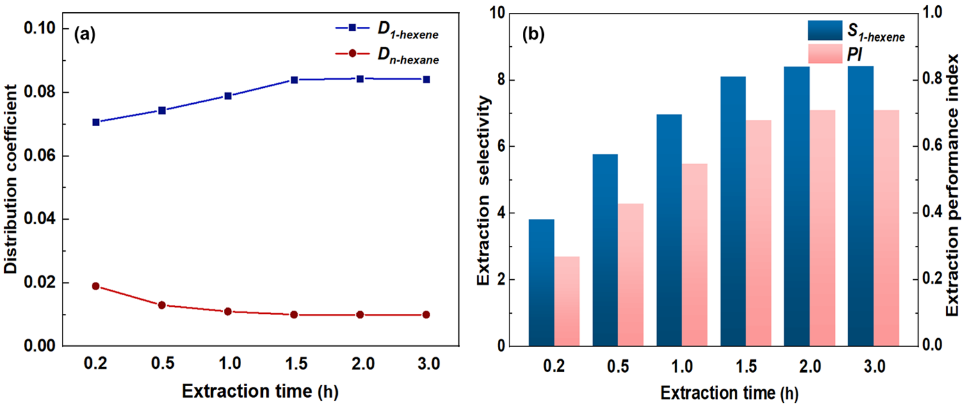

Figure 7. Influence of extraction time on (a) the distribution coefficient, (b) the extraction selectivity, and the extraction performance index of 1-hexene.

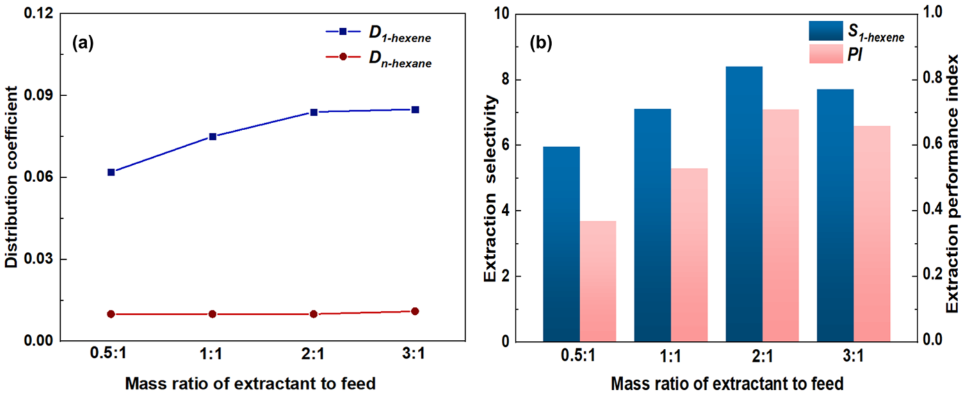

Figure 8. Influence of the mass ratio of extractant to feed on (a) the distribution coefficient, (b) the extraction selectivity, and the extraction performance index of 1-hexene.

an auxiliary effect. However, chemical complexation was very sensitive to temperature changes. Since the complexation was exothermic, increasing temperature would make the equilibrium shift to the endothermic direction, which was not conducive to the complexation of bimetallic ionic liquid and 1-hexene and reduced the extraction effect. It could be seen from the experimental results that increasing the temperature was obviously unfavorable to extraction, so the importance of chemical complexation in the extraction process was further demonstrated. However, lower temperatures were not always better, and the viscosity of the Fe−Cu bimetallic ionic liquid increased significantly and even reached 1050 cP at 5 °C (Table S6 and Figure S3). The high viscosity with a temperature below 10 °C would affect the heat and mass transfer of the extraction process. In conclusion, bimetallic ionic liquid has an excellent olefin extraction effect and suitable viscosity at 10 °C, which would be the optimal extraction temperature.

3.3.2. Effect of Extraction Time.

The effect of the extraction time on the separation was investigated. The extraction pressure, extraction temperature, mass ratio of 1-hexene to *n*-hexane, and mass ratio of extractant to feed were 1 atm, 10 °C, 1:1, and 2:1, respectively. Figure 7 depicts that with the extension of extraction time, the distribution coefficient, extraction performance index, and selectivity of 1-hexene all showed a trend of increasing at first and then maintaining a constant. This was mainly due to the long extraction time that could be conducive to the full contact between Fe−Cu bimetallic ionic liquid and 1-hexene and then was conducive to the complex of 1-hexene. In addition, $D_{n\text{-hexane}}$ showed a trend of decreasing first and then maintaining a constant. Since 1-hexene gradually existed in a relatively large amount in Fe−Cu bimetallic ionic liquids through long extraction time, it would occupy the "capacity" of the bimetallic ionic liquid. The Fe−Cu bimetallic ionic liquid was gradually saturated, and the dissolution capacity to *n*-hexane decreased, resulting in a decline in the distribution coefficient of *n*-hexane until extraction equilibrium. With the extraction time above 2 h, the extraction selectivity and extraction performance indexes remained unchanged, and the complete extraction equilibrium was achieved.

3.3.3. Effect of the Mass Ratio of Extractant to Feed.

The effect of the mass ratio of the extractant to feed on the separation was investigated. The extraction pressure, extraction temperature, extraction time, and mass ratio of 1-hexene to *n*-hexane were 1 atm, 10 °C, 2 h, and 1:1, respectively. Figure 8 showed that as the mass ratio of extractant to feed increased, the amount of bimetallic ionic liquid increased, the more complex sites could be provided, and $D_{1\text{-hexene}}$ increased. In addition, the increase in $D_{n\text{-hexane}}$ was not significant, which led to an increase in the extraction selectivity and the extraction performance index. When the mass ratio of extractant to feed was 3:1, although the concentration of 1-hexene in the extraction phase increased, the increase in $D_{1\text{-hexene}}$ was not significant. In addition, the amount of dissolved *n*-hexane increased with the increase of bimetallic ionic liquid, which led

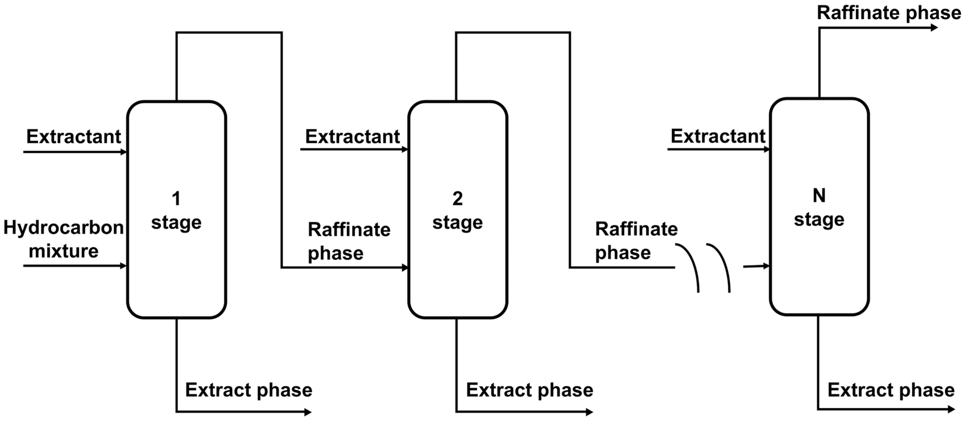

Figure 9. Flowchart of N-stage extraction.

Table 4. Phase Equilibrium Data of 1-Hexene (1)/*n*-Hexane (2)−Fe-Cu Bimetallic Ionic Liquid (3) Systems and the Extraction Selectivity, Extraction Performance Index of 1-Hexene in the Systems at 10 °C from Stage 1 to Stage 5

	hydrocarbon-rich phase			ionic liquid-rich phase				
stage	x_1	x_2	x_3	x_1	x_2	x_3	$S_{1\text{-hexene}}$	PI
1	46.50	53.50	0.00	3.95	0.54	95.51	8.41	0.71
2	43.30	56.70	0.00	3.73	0.58	95.69	8.42	0.73
3	40.20	59.80	0.00	3.40	0.59	96.01	8.57	0.73
4	37.30	62.70	0.00	3.40	0.66	95.94	8.66	0.79
5	34.85	65.15	0.00	3.31	0.71	95.98	8.72	0.83

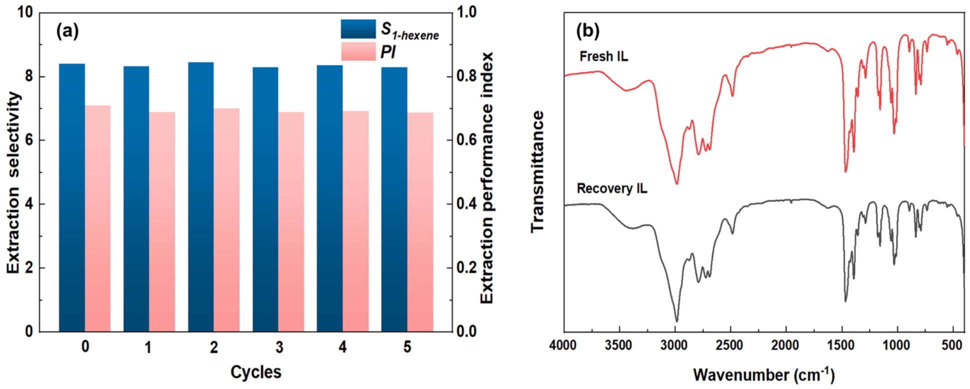

Figure 10. (a) Recycling of bimetallic ionic liquid; (b) FT-IR spectra of fresh Fe−Cu bimetallic ionic liquid and recovery Fe−Cu bimetallic ionic liquid.

to a decrease in the extraction selectivity and the extraction performance index. At the mass ratio of 2:1, the extraction selectivity reached 8.41, and the extraction performance index was 0.71. The extraction efficiency of 1-hexene was improved by the appropriate mass ratio of extractant to feed.

3.4. Sequential Liquid−Liquid Extraction. Although the Fe−Cu bimetallic ionic liquid showed high extraction selectivity for 1-hexene, its solubility for 1-hexene was relatively low. Sequential liquid−liquid extraction can achieve the accumulation of the product yield. The process of sequential liquid−liquid extraction is shown in Figure 9. The liquid−liquid equilibrium data, extraction selectivity, and extraction performance index of 1-hexene were analyzed (Table 4). After 5 stages of extraction, the purity of 1-hexene exceeded 85%, and the yield exceeded 50%.

Sequential liquid−liquid extraction stage optimization is the key to improving the efficiency and economy of the extraction process. In industrial applications, it is necessary to determine the optimal extraction stage through experiment and simulation. The product purity, yield, extractant dosage, and energy consumption should be comprehensively considered. Diminishing returns are a common phenomenon in sequential liquid−liquid extraction, and the overall separation effect is improved by optimizing operating conditions, using efficient mixing equipment, applying multistage counter-current extraction, and introducing washing or concentration steps between key stages. The amplification effect is one of the challenges of sequential liquid−liquid extraction on an industrial scale. Laboratory data may be inaccurate for equipment enlargement due to changes in fluid dynamics and mass transfer efficiency. Pilot tests and mathematical models are needed to predict the effect of scale-up. In terms of operational stability, fluctuations in continuous production may lead to unstable product quality, requiring the design of buffer tanks and real-time monitoring systems. Solvent loss and recovery costs are significant in the industry. Recycling

Table 5. Extraction Performance of 1-Hexene Using Traditional Organic Extractants, Deep Eutectic Solvents, and Ionic Liquids

extractant	temperature (°C)	concentration of olefins	volume ratio of extractant to feed	$S_{1\text{-hexene}}$
γ-butyrolactone[15]	25	0.4	1	2.0
N-formylmorpholine[15]	30	0.6	1	2.3
1-methylimidazole[15]	30	0.5	1	2.3
$[Bmim][NTf_2]$[12]	30	0.5	1	2.2
$[Emim][N(CN)_2]$[12]	30	0.5	1	2.6
$[CONmim][NTf_2]$[12]	30	0.5	1	2.9
$[Bmim]NTf_2$-$AgNTf_2$ [0.25 M][12]	30	0.5	1	3.4
$[Ag(DMBA)_2][NTf_2]$[41]	20	0.5	0.1	4.4
$[Ag(PrNH_2)_2][NTf_2]$[41]	20	0.5	0.1	1.1
TBAB/TEG (1/4)[14]	25	0.2	2.2	2.5
ChCl/DEG (1/4)[14]	25	0.2	1.8	1.5
TBAB/LA (1/2)[14]	25	0.2	3	1.7
Et_3NHCl–$0.47FeCl_3$–$0.8CuCl$ (this work)	20	0.5	0.1	3.9
Et_3NHCl–$0.47FeCl_3$–$0.8CuCl$ (this work)	30	0.5	1	6.2
Et_3NHCl–$0.47FeCl_3$–$0.8CuCl$ (this work)	10	0.5	1	8.4

When the volume ratio of Et_3NHCl-$0.47FeCl_3$-$0.8CuCl$ to feed was 1:1, the mass ratio of Et_3NHCl-$0.47FeCl_3$-$0.8CuCl$ to feed was approximately 2:1.

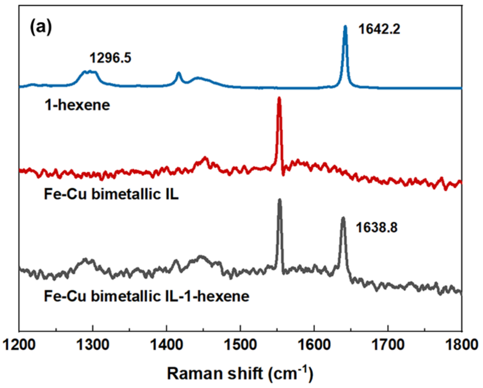

Figure 11. Raman spectra of (a) Fe–Cu bimetallic IL and 1-hexene and their complex; (b) Fe–Cu bimetallic IL and *n*-hexane and their complex.

extractants is a good way to reduce the use of extractants. Therefore, recycling experiments were performed to investigate the recycling performance of the Fe–Cu bimetallic ionic liquid.

3.5. Recycle of Extractants. An important index is the cyclic stability during the extraction of 1-hexene by an Fe–Cu bimetallic ionic liquid. Five consecutive recycling experiments were performed (Figure 10). The extract phase was distilled by a distillation apparatus at atmospheric pressure under the protection of N_2 and 100 °C for 1 h (Figure S4). The extraction selectivity and the extraction performance index of each cycle varied slightly. In addition, after five absorption–desorption cycles, the vibration peaks of characteristic groups in the FT-IR spectra of Fe–Cu bimetallic ionic liquids had no significant changes compared with those of fresh Fe–Cu bimetallic ionic liquids. Based on the results above, the Fe–Cu bimetallic ionic liquid had good cyclic stability for the extraction of 1-hexene.

3.6. Comparison with Other Extractants. The extraction performance of ILs, deep eutectic solvent (DES), and traditional organic extractants is summarized in Table 5. The Fe–Cu bimetallic ionic liquid showed obvious separation advantages compared with other extractants reported in the literature. For the traditional organic extractants, the extraction selectivity was about 2. The interaction of organic solvents with olefins was related to van der Waals force. For the conventional ionic liquids and functional group-containing ionic liquids, most of them showed good extraction selectivity due to van der Waals force and weak hydrogen bond. The extraction performances of DESs were also related to van der Waals force and weak hydrogen bonds, and the extraction selectivity was about 2. $[Ag(DMBA)_2][NTf_2]$ showed better extraction selectivity, mainly due to the complexation of Ag^+ with 1-hexene. Respectively, under similar extraction conditions, the extraction selectivity of the Fe–Cu bimetallic ionic liquid was 3.9–8.4, which had high extraction selectivity compared with traditional organic extractants and ionic liquids. The Fe–Cu bimetallic ionic liquid was easier to produce and less expensive, making this method more economical.

3.7. Raman Analysis. Raman spectroscopy provides molecular vibrational information, which can reflect the structural changes caused by the interaction between molecules. The interaction of Fe–Cu bimetallic ionic liquid $[Et_3NH]Cl$–$0.47FeCl_3$–$0.8CuCl$ with 1-hexene and *n*-hexane was analyzed by Raman spectroscopy. As depicted in Figure 11, the spectrum of the $[Et_3NH]Cl$–$0.47FeCl_3$–$0.8CuCl$-1-hexene complex was compared with those of $[Et_3NH]Cl$–$0.47FeCl_3$–$0.8CuCl$ and 1-hexene. It was found that the peak at 1296.5 cm^{-1} of 1-hexene appeared in the complex spectrum. This indicated that 1-hexene dissolved $[Et_3NH]Cl$–$0.47FeCl_3$–$0.8CuCl$. In the spectrum of 1-hexene, the

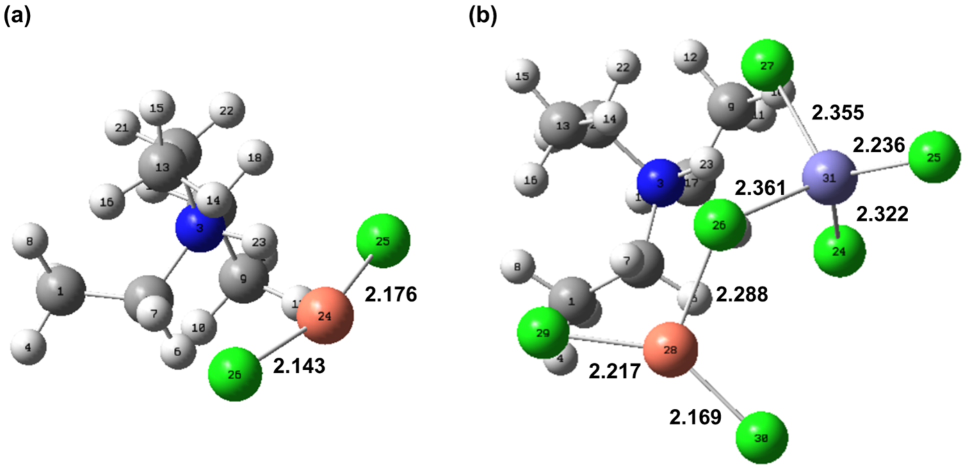

Figure 12. Optimized structure of (a) Cu-based IL; (b) Fe—Cu bimetallic IL (N: blue; H: white; C: gray; Cl: green; Cu: orange; Fe: mauve).

stretching vibration peak of the C═C was found at 1642.2 cm^{-1}, and a peak was also found at 1638.8 cm^{-1} in the $[Et_3NH]Cl-0.47FeCl_3-0.8CuCl$-1-hexene complex spectrum. The double bond peak of 1-hexene had a slight red shift, possibly related to the chemical complexation occurring on the double bond. The chemical environment was affected by cuprous ions, the intensity of the double bond peak was reduced, and the direction of low energy was shifted. For the spectrum of $[Et_3NH]Cl-0.47FeCl_3-0.8CuCl$-*n*-hexane, the two peaks of 1139.8 and 1302.2 cm^{-1} of *n*-hexane did not appear, which suggested that *n*-hexane and $[Et_3NH]Cl-0.47FeCl_3-0.8CuCl$ were nearly immiscible. The extraction experimental results showed that a small amount of *n*-hexane could be dissolved in the Fe—Cu bimetallic ionic liquid, which was difficult to detect because of its low concentration. In summary, the interaction between Fe—Cu bimetallic ionic liquid and 1-hexene involved physical dissolution and chemical complexation. The excellent extractant for separating 1-hexene and *n*-hexane should have strong chemical complexation and physical dissolution to 1-hexene rather than to *n*-hexane.

3.8. Quantum Chemistry Calculation. Quantum chemistry calculation is widely used in the fields of exploring interaction mechanisms and separation mechanisms,[42,43] providing theoretical support for experiments and promoting scientific research and technological development. In this study, the structures were optimized based on density functional theory (DFT), and the charge transfer of Fe—Cu bimetallic ionic liquids was revealed. The strength of the interaction was evaluated by calculating the interaction energy between the Fe—Cu bimetallic ionic liquid and 1-hexene/*n*-hexane. The interaction of Fe—Cu bimetallic ionic liquid with 1-hexene/*n*-hexane was graphically demonstrated by IGMH analysis.[44] The atomic interaction was studied by AIM analysis,[45] and the interaction between Fe—Cu bimetallic ionic liquid and 1-hexene/*n*-hexane was further discussed.

3.8.1. Geometric Structures. To reveal that the effect of Fe—Cu bimetallic IL extraction of 1-hexene was significantly improved, the structures of Cu-based IL and Fe—Cu bimetallic IL were optimized (Figure 12). In Cu-based IL, the primary anion was $[CuCl_2]^-$, with bond lengths of Cu—Cl_{25} and Cu—Cl_{26} measuring 2.176 and 2.143 Å. In Fe—Cu bimetallic IL, the bond lengths of Cu—Cl_{29} were 2.217 Å, and those of Cu—Cl_{30} were 2.169 Å, indicating that Cu—Cl bonds weakened in the Fe—Cu bimetallic ionic liquid. Notably, the bond length of Cu—Cl_{26}, which was 2.288 Å, fell below the sum of the van der Waals radii of Cu (1.57 Å) and Cl (1.75 Å), indicating the interaction between Cu^+ and Cl_{26} ions. The bond length of Cu—Cl_{26} (2.288 Å) was larger than Cu—Cl_{29} and Cu—Cl_{30} (2.217 Å, 2.169 Å) of $[CuCl_2]^-$, suggesting that a moderate interaction was observed between Cu^+ and Cl_{26} ions. The charge density of Cu^+ in Cu-based IL and Fe—Cu bimetal IL was further calculated (Figure 13), the charge density of Cu^+ increased from +0.385 to +0.546e, and the bond energy decreased from 119.10 to 93.18 kJ·mol^{-1}, suggesting that the Cu^+ in Fe—Cu bimetallic IL had greater chemical activity. The enhancement in the charge density of Cu^+ correlated with the elongation of bond lengths between Cu^+ and Cl^-. Therefore, the introduction of Fe^{3+} weakened the electrostatic interaction between Cu^+ and Cl^-, and electron transfer between CuCl and $FeCl_3$ increased the activation of Cu^+.

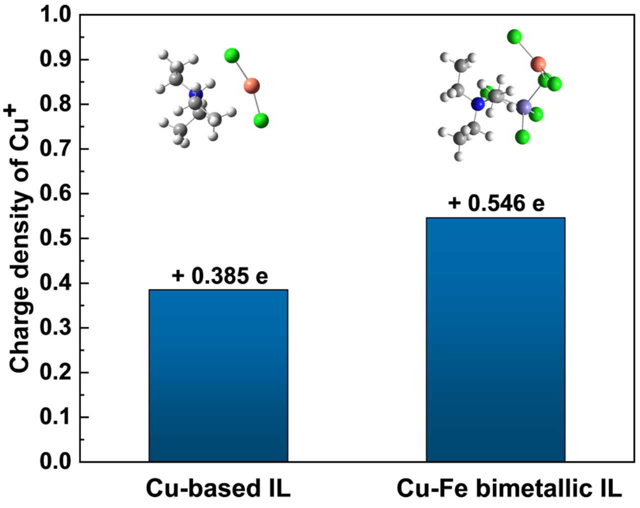

Figure 13. Charge densities of Cu^+ in Cu-based IL and Fe—Cu bimetallic IL (N: blue; H: white; C: gray; Cl: green; Cu: orange; Fe: mauve).

3.8.2. Interaction Energy Analysis. To explore the interaction between Fe—Cu bimetallic ILs and 1-hexene/*n*-hexane from a quantum chemistry perspective, their relative positions were optimized. The optimized Fe—Cu bimetallic ILs with 1-hexene and *n*-hexane were subjected to interaction energy analysis (Table 6). The interaction energy of the Fe—

Table 6. Interaction Energies of Ionic Liquids with 1-Hexene/*n*-Hexane

IL + hydrocarbon	ΔE (kJ·mol^{-1})
Fe−Cu bimetallic IL + 1-hexene	−109.74
Fe−Cu bimetallic IL + *n*-hexane	−12.19
Cu-based IL + 1-hexene	−71.34
Cu-based IL + *n*-hexane	−15.62

Cu bimetallic ionic liquid with 1-hexene considering BSSE correction was −109.74 kJ·mol^{-1}, and its absolute value was far greater than that with *n*-hexane. The larger interaction energy difference determined that 1-hexene had higher solubility in Fe−Cu bimetallic ionic liquid, which was favorable for the separation of olefins by bimetallic ionic liquids (Table S9 and Figure S5). Furthermore, the addition of $FeCl_3$ into a Cu-based IL (Figure S10) increased the interaction energy between 1-hexene and ILs from −71.34 to −109.74 kJ·mol^{-1}. This enhanced the separation effect by the Fe−Cu bimetal IL and reflected the activation of Cu$^+$.

3.8.3. IGMH Analysis. To intuitively analyze the weak interaction between Fe−Cu bimetallic ILs and 1-hexene/*n*-hexane, we utilized the independent gradient model of Hirshfeld partitioning (IGMH). IGMH is an IGM method based on the partitioning of the molecular density of Hirshfeld, and the use of IGMH can shield the interactions between anions and cations of ILs, which is beneficial for the analysis of weak interactions. The IGMH result is shown in Figure 14. It could be observed that the Cu$^+$ of the bimetallic ionic liquid had a strong mutual attraction with C_{32} and C_{33} near Cu on 1-hexene. Among all d-region elements, Cu had the $(n-1)d^{10}ns^0$ electronic configuration, which was easy to accept electrons and to give d-electrons, so the d orbitals of Cu in the bimetallic ionic liquid overlap with the π-orbitals of C_{32} and C_{33} on 1-hexene, and then, 1-hexene could interact with Cu$^+$ in the bimetallic ionic liquids by π-bond complexation, which achieved high selectivity and led to efficient separation. In addition, there was a weak interaction between the methyl H of 1-hexene and the Cl of the Fe−Cu bimetallic ionic liquid, and the balance of the above interactions allowed the complex to stabilize.

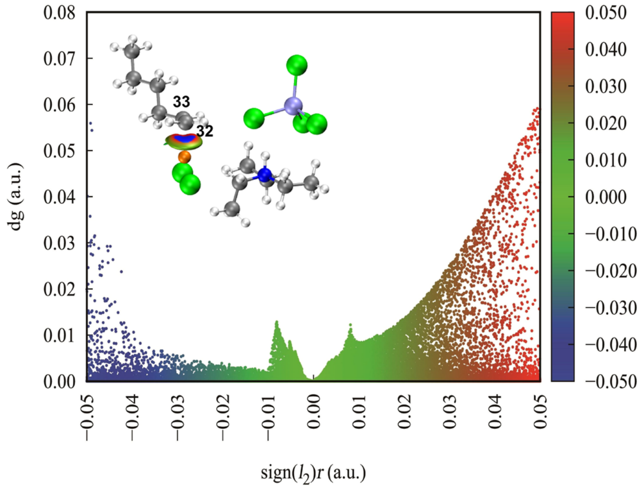

Figure 14. IGMH diagram of the Fe−Cu bimetallic ionic liquids and 1-hexene (N, blue; H, white; C, gray; Cl: green; Cu: orange; Fe: mauve. The blue color signified the low contribution, and the red color denoted the high contribution.).

For Fe−Cu bimetallic ionic liquid and *n*-hexane, the interaction was mainly concentrated between Cl of the bimetallic ionic liquid and the methyl H of the *n*-hexane, suggesting that there was a weak interaction between them (Figure S7). The results indicated that the interaction form and interaction region between Fe−Cu bimetallic IL and 1-hexene was significantly different from that between Fe−Cu bimetallic IL and *n*-hexane. The Fe−Cu bimetallic ionic liquid could selectively complex 1-hexene in the mixing system and then achieve the purpose of selective separation of 1-hexene.

3.8.4. AIM Analysis. To further explore the interaction between Fe−Cu bimetallic IL and hydrocarbons, the interaction of atoms was analyzed by atoms in molecule (AIM). AIM theory puts forward the concept of the bond critical point (BCP), which is equivalent to the point of modulus zero of the gradient of a function, generally referring to the function of electron density. BCP can be divided into four types: (3, −3), (3, −1), (3, +1), and (3, +3), among which the properties of type (3, −1) BCP are commonly used to examine the essential characteristics of the corresponding chemical bond. A set of topological parameters of type (3, −1) BCPs in Fe−Cu bimetallic ionic liquids with 1-hexene/*n*-hexane were calculated (Tables 7 and S10). In this case, H(BCP) was used to distinguish covalent and noncovalent interactions, and ρ(BCP) was used to determine hydrogen bonds and non-hydrogen bonds.[46]

Table 7. Part Parameters of BCPs in Fe−Cu Bimetallic Ionic Liquids with 1-Hexene/*n*-Hexane

types	BCP	bonds	ρ(BCP)	$\nabla^2\rho$(BCP)	H(BCP)
coordination bond	1	Cu···C	0.0784	0.3048	−0.0115
weak hydrogen bond	3	C−H···Cl	0.0082	0.0283	0.0010
	8	C−H···Cl	0.0136	0.0344	0.0001
	15	C−H···Cl	0.0037	0.0141	0.0008
	20	C−H···Cl	0.0075	0.0226	0.0005
	26	C−H···Cl	0.0078	0.0236	0.0007
	32	C−H···Cl	0.0091	0.0262	0.0005
covalent bond	5	Cu···Cl	0.0609	0.2504	−0.0034

As depicted in Figure 15, the corresponding BCPs were present in the region of interfragment interaction in the IGMH analysis described above. Fe−Cu bimetallic IL was bound to 1-hexene/*n*-hexane, and multiple C−H···Cl bonds between the anion and cation facilitated stabilizing the Fe−Cu bimetallic IL structure. For the BCP parameters of the Cu···C bond, ρ(BCP) was 0.0784, $\nabla^2\rho$(BCP) was 0.3048, and H(BCP) was −0.0115. ρ(BCP) parameter for the Cu···C linkage exhibited a modestly positive value, which pointed to a feeble interaction existing between the Cu$^+$ and C atoms. A positive value was observed for $\nabla^2\rho$(BCP), revealing a decrement in electron density and emphasizing the ionic nature of bonds. Conversely, the H(BCP) value demonstrated a negative sign, which denoted the presence of covalent bond features within these bonds. This suggested that Cu···C was the π-bond complexation that corresponds to a coordination bond. When Fe−Cu bimetallic IL combined with *n*-hexane, there were mainly C−H···Cl bonds; ρ(BCP), $\nabla^2\rho$(BCP), and H(BCP) were all positive, but the values were significantly lower, which

https://doi.org/10.1021/acsomega.5c00224
ACS Omega 2025, 10, 17744−17757

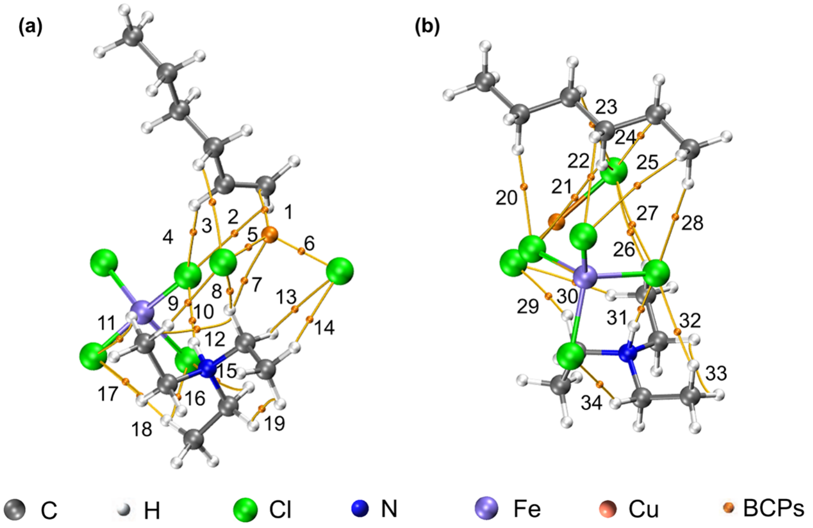

Figure 15. AIM analysis for (a) Fe−Cu bimetallic ionic liquids +1-hexene; (b) Fe−Cu bimetallic ionic liquids + *n*-hexane.

further revealed that Fe−Cu bimetallic ILs with *n*-hexane were mainly weak hydrogen bonds.

4. CONCLUSIONS

The novel bimetallic ionic liquid extractants for 1-hexene/*n*-hexane separation were synthesized. The appropriate proportions of $FeCl_3$ and CuCl in bimetallic ionic liquids could improve the extraction effect. $[Et_3NH]Cl-0.47FeCl_3-0.8CuCl$ showed good extraction performance, and under the optimal extraction temperature, extraction time, and mass ratio of extractant to feed which was 10 °C, 2 h, and 2:1, respectively, a high olefin selectivity (8.41) and a high extraction performance index (0.71) were achieved. Through 5 extraction stages, the purity of 1-hexene exceeded 85%, and the yield exceeded 50%. Fe−Cu bimetallic ionic liquids possessed a higher selectivity in the separation of 1-hexene/*n*-hexane than those traditional organic solvents and ionic liquids reported by previous researchers. Quantum chemistry calculations showed that the electron transfer between $[CuCl_2]^-$ and $[FeCl_4]^-$ increased the activity of Cu^+. In addition, Raman analysis, interaction energies, IGMH analysis, and AIM analysis showed that there were chemical complexation and weak hydrogen bonds between bimetallic ionic liquid and 1-hexene, while the interaction between bimetallic ionic liquid and *n*-hexane was weak. The large difference in interaction between 1-hexene and *n*-hexane with bimetallic ILs determined the good extraction performance. Five recycling experiments showed good recycling performance of the bimetallic ionic liquid.

Bimetallic ionic liquid, as a new designable green extractant, has great application potential in the separation of olefin/alkane. In future studies, the stability of bimetallic ionic liquids in long-period experiments needs to be further explored. It is necessary to further optimize the composition and regulate the structural characteristics of bimetallic ionic liquid to improve the extraction effect. In addition, we explore more efficient separation processes and develop the appropriate theoretical model, which provides the possibility for the industrial application of bimetallic ionic liquids.

■ ASSOCIATED CONTENT

Supporting Information

The Supporting Information is available free of charge at https://pubs.acs.org/doi/10.1021/acsomega.5c00224.

> Repeatability verification of 1-hexene/*n*-hexane by bimetallic ionic liquids (Table S1). The complete data for density and viscosity (Tables S2−S6). The fitting data for density (Table S7) and viscosity (Table S8) versus temperature; energies of isolated molecules, ILs, and their cluster (Table S9); parameters of BCPs in Fe−Cu bimetallic ionic liquids with 1-hexene/*n*-hexane (Table S10); FT-IR spectra and Raman spectra of metal ionic liquids (Figures S1 and S2); effect of viscosities and densities of $[Et_3NH]Cl-0.47FeCl_3$-0.8CuCl (Figure S3); flowchart of extract recycle (Figure S4); structure of Fe−Cu bimetallic IL and 1-hexene, Fe−Cu bimetallic IL and *n*-hexane (Figure S5); structure of Cu-based IL and 1-hexene and Cu-based IL and *n*-hexane (Figure S6); and IGMH diagram of the bimetallic ionic liquids and *n*-hexane (Figure S7). (PDF)

■ AUTHOR INFORMATION

Corresponding Authors

Rui Zhang − *State Key Laboratory of Heavy Oil Processing, China University of Petroleum, Beijing 102249, China*; Email: zr@cup.edu.cn

Xianghai Meng − *State Key Laboratory of Heavy Oil Processing, China University of Petroleum, Beijing 102249, China*; orcid.org/0000-0001-9494-6996; Email: mengxh@cup.edu.cn

Authors

Jiaxin Cui − *State Key Laboratory of Heavy Oil Processing, China University of Petroleum, Beijing 102249, China*

Mengfan Yin − *State Key Laboratory of Heavy Oil Processing, China University of Petroleum, Beijing 102249, China*

Tao Zheng − *State Key Laboratory of Heavy Oil Processing, China University of Petroleum, Beijing 102249, China*

Han Liu − *State Key Laboratory of Heavy Oil Processing, China University of Petroleum, Beijing 102249, China*

Haiyan Liu − *State Key Laboratory of Heavy Oil Processing, China University of Petroleum, Beijing 102249, China*

Zhichang Liu − *State Key Laboratory of Heavy Oil Processing, China University of Petroleum, Beijing 102249, China*; orcid.org/0000-0001-7418-8104

Chunming Xu − *State Key Laboratory of Heavy Oil Processing, China University of Petroleum, Beijing 102249, China*

Complete contact information is available at: https://pubs.acs.org/10.1021/acsomega.5c00224

Notes

The authors declare no competing financial interest.

ACKNOWLEDGMENTS

The authors gratefully acknowledge the financial support of the National Natural Science Foundation of China (22021004 and 22078359).

REFERENCES

(1) Doosti, M.; Abedini, R. Polyethyleneglycol-Modified Cellulose Acetate Membrane for Efficient Olefin/Paraffin Separation. *Energy Fuels* **2022**, *36*, 10082−10095.

(2) Li, Y.; Li, L.; Zhao, H.; Liu, J.; Zhu, K. Ag^+ anchored on sulfonic functionalized mesoporous silica towards efficient liquid phase Olefin-Paraffin separation. *Sep. Purif. Technol.* **2023**, *322*, No. 124276.

(3) Sholl, D. S.; Lively, R. P. Seven chemical separations to change the world. *Nature* **2016**, *532*, 435−437.

(4) Syauqi, A.; Kim, H.; Lim, H. Optimizing olefin purification: An artificial intelligence-based process-conscious PI controller tuning for double dividing wall column distillation. *Chem. Eng. J.* **2024**, *500*, No. 156645.

(5) Yang, R.; Gao, R.; Wang, Y.; Qian, Z.; Luo, G. Selective Adsorption of C_6, C_8, and C_{10} Linear α-Olefins from Binary Liquid-Phase Olefin/Paraffin Mixtures Using Zeolite Adsorbents: Experiment and Simulations. *Langmuir* **2020**, *36*, 8597−8609.

(6) Liu, J.; Zhao, S.; Chen, X.; Shen, B. Upgrading FCC gasoline through adsorption separation of normal hydrocarbons. *Fuel* **2016**, *166*, 467−472.

(7) Kumar, A.; Zhou, T.; Emge, T. J.; Mironov, O.; Saxton, R. J.; Krogh-Jespersen, K.; Goldman, A. S. Dehydrogenation of n-Alkanes by Solid-Phase Molecular Pincer-Iridium Catalysts. High Yields of α-Olefin Product. *J. Am. Chem. Soc.* **2015**, *137*, 9894−9911.

(8) Gala, A.; Guerrero, M.; Guirao, B.; Domine, M. E.; Serra, J. M. Characterization and Distillation of Pyrolysis Liquids Coming from Polyolefins Segregated of MSW for Their Use as Automotive Diesel Fuel. *Energy Fuels* **2020**, *34*, 5969−5982.

(9) Lei, Y.; Pan, W.; Hu, S.; Kuang, Y.; Liu, X.; Chen, Y. Ionic Liquid-Assisted Extractive Distillation for Ethylene/Ethane Separation: Molecular Design and Process Assessment. *Ind. Eng. Chem. Res.* **2024**, *63*, 19187−19199.

(10) Wang, K.; Ren, Y.; Luo, J.; Zhuang, Y.; Feng, S.; Wan, Y. Highly Stable Silver-Loaded Membrane Prepared by Interfacial Polymerization for Olefin Separation. *Ind. Eng. Chem. Res.* **2022**, *61*, 11922−11933.

(11) Deng, R.; Sun, Y.; Bi, H.; Dou, H.; Yang, H.; Wang, B.; Tao, W.; Jiang, B. Deep Eutectic Solvents As Tuning Media Dissolving Cu^+ Used in Facilitated Transport Supported Liquid Membrane for Ethylene/Ethane Separation. *Energy Fuels* **2017**, *31*, 11146−11155.

(12) Li, R.; Xing, H.; Yang, Q.; Zhao, X.; Su, B.; Bao, Z.; Yang, Y.; Ren, Q. Selective Extraction of 1-Hexene Against n-Hexane in Ionic Liquids with or without Silver Salt. *Ind. Eng. Chem. Res.* **2012**, *51*, 8588−8597.

(13) Das, D.; Biswas, S.; Rao Dumpala, R. M.; Pente, A. S.; Manohar, S. Separation of Radioactive Ruthenium from Alkaline Solution: A Solvent Extraction and Detailed Mechanistic Approach. *ACS Omega* **2022**, *7*, 43803−43812.

(14) El blidi, L.; Hadj-Kali, M. K.; Al-Anazi, A. M.; Alhawtali, S. M.; Wazeer, I. Liquid-liquid separation of n-hexane/1-hexene and cyclohexane/cyclohexene using deep eutectic solvents. *J. Mol. Liq.* **2021**, *344*, No. 117776.

(15) Zhu, L.; Li, F.; Zhu, J.; Lei, Z. Liquid-liquid equilibria of ternary systems of 1-hexene/hexane and extraction solvents. *Chem. Pap.* **2016**, *0*, 585−593.

(16) Cheng, Y.; Li, F.; Wu, Q.; Peng, K.; Fan, B.; Bai, Y.; Wang, Z.; Zhang, N.; Zhang, X. Efficient ethylene/ethane separation by rare earth metal-containing ionic liquids in N,N-dimethylformamide. *Sep. Purif. Technol.* **2023**, *310*, No. 123094.

(17) Lei, Y.; Guo, Z.; Du, L.; Meng, X.; Liu, X.; Wu, X.; Chen, Y. Replacing DMF with ionic liquid in isoprene/n-pentane separation in C5 plants: Solvent design, process optimization, and industrial-scale assessment. *Fuel* **2024**, *357*, No. 130006.

(18) Ryoo, D.; Eor, P.; Bara, J. E.; Anderson, J. L. Comparison of olefin/paraffin separation by ionic liquid and polymeric ionic liquid stationary phases containing silver(I) ion using one-dimensional and multidimensional gas chromatography. *J. Chromatogr. A* **2023**, *1698*, No. 463996.

(19) Mortaheb, H. R.; Mafi, M.; Mokhtarani, B.; Sharifi, A.; Mirzaei, M.; Khodapanah, N.; Ghaemmaghami, F. Experimental kinetic analysis of ethylene absorption in ionic liquid $[Bmim]NO_3$ with dissolved $AgNO_3$ by a semi-continuous process. *Chem. Eng. J.* **2010**, *158*, 384−392.

(20) Fallanza, M.; Ortiz, A.; Gorri, D.; Ortiz, I. Propylene and Propane Solubility in Imidazolium, Pyridinium, and Tetralkylammonium Based Ionic Liquids Containing a Silver Salt. *J. Chem. Eng. Data* **2013**, *58*, 2147−2153.

(21) Wu, Q.; Li, G.; Cheng, Y.; Fan, B.; Bai, Y.; Zhang, N.; Wang, Z.; Zhang, X.; Zhang, S. Efficient separation of ethylene/ethane by incorporation of silver salts into protic imidazole ionic liquids. *Chem. Eng. J.* **2023**, *461*, No. 141942.

(22) Yu, G.; Deng, L.; Abdeltawab, A. A.; Al-Deyab, S. S.; Chen, X.; Zhang, J. Functional Solution Composed of Cu(I) Salt and Ionic Liquids to Separate Propylene from Propane. *Ind. Eng. Chem. Res.* **2014**, *53*, 13430−13435.

(23) Yu, G.; Zhang, L.; Alhumaydhi, I. A.; Abdeltawab, A. A.; Bagabas, A. A.; Al-Megren, H. A.; Al-Deyab, S. S.; Chen, X. Separation of propylene and propane by alkylimidazolium thiocyanate ionic liquids with Cu^+ salt. *Sep. Purif. Technol.* **2015**, *156*, 356−362.

(24) Kore, R.; Kelley, S. P.; Aduri, P.; Rogers, R. D. Mixed metal double salt ionic liquids comprised of $[HN_{222}]_2[ZnCl_4]$ and $AlCl_3$ provide tunable Lewis acid catalysts related to the ionic environment. *Dalton Trans.* **2018**, *47*, 7795−7803.

(25) González-Martín, R.; Jullakan, S.; Trujillo-Rodríguez, M. J.; Abbasi, N. M.; De Silva, S.; Anderson, J. L.; Pino, V. Exploring a new generation of bimetallic magnetic ionic liquids with ultra-low viscosity in microextraction that enable direct coupling with high-performance liquid-chromatography. *Anal. Chim. Acta* **2024**, *1301*, No. 342448.

(26) Li, Z.; Wang, Z.; Cao, D.; Shi, Y.; Zhao, Y.; Wang, H.; Wang, J. Designing bimetallic ionic liquid hybridized molecular sieve adsorbents for efficient ammonia adsorption at high temperature and low content. *Sep. Purif. Technol.* **2025**, *354*, No. 128861.

(27) Kobayashi, S.; Busujima, T.; Nagayama, S. A Novel Classification of Lewis Acids on the Basis of Activity and Selectivity. *Chem. − Eur. J.* **2000**, *6*, 3491−3494.

(28) Jiang, B.; Tao, W.; Dou, H.; Sun, Y.; Xiao, X.; Zhang, L.; Yang, N. A Novel Supported Liquid Membrane Based on Binary Metal Chloride Deep Eutectic Solvents for Ethylene/Ethane Separation. *Ind. Eng. Chem. Res.* **2017**, *56*, 15153−15162.

(29) Frisch, M. J.; Trucks, G. W.; Schlegel, H. B.; Scuseria, G. E.; Robb, M. A.; Cheeseman, J. R.; Scalmani, G.; Barone, V.; Mennucci, B.; Petersson, G. A. *Gaussian 09*, revision E.01; Gaussian, Inc.: Wallingford, CT, 2009.

(30) Adamo, C.; Barone, V. Toward reliable density functional methods without adjustable parameters: The PBE0 model. *J. Chem. Phys.* **1999**, *110*, 6158−6170.

(31) Zheng, J.; Xu, X.; Truhlar, D. G. Minimally augmented Karlsruhe basis sets. *Theor. Chem. Acc.* **2011**, *128*, 295−305.

(32) Grimme, S.; Ehrlich, S.; Goerigk, L. Effect of the damping function in dispersion corrected density functional theory. *J. Comput. Chem.* **2011**, *32*, 1456−1465.

(33) Goerigk, L.; Grimme, S. Efficient and Accurate Double-Hybrid-Meta-GGA Density Functionals—Evaluation with the Extended GMTKN30 Database for General Main Group Thermochemistry, Kinetics, and Noncovalent Interactions. *J. Chem. Theory Comput.* **2011**, *7*, 291−309.

(34) Li, H.; Sun, G.; Li, D.; Xi, L.; Zhou, P.; Li, X.; Zhang, J.; Gao, X. Molecular interaction mechanism in the separation of a binary azeotropic system by extractive distillation with ionic liquid. *Green Energy Environ.* **2021**, *6*, 329−338.

(35) Neese, F. Software update: the ORCA program system, version 4.0. *WIREs Comput. Mol. Sci.* **2018**, *8*, No. e1327.

(36) Lu, T.; Chen, F. Multiwfn: A multifunctional wavefunction analyzer. *J. Comput. Chem.* **2012**, *33*, 580−592.

(37) Humphrey, W.; Dalke, A.; Schulten, K. VMD. Visual molecular dynamics. *J. Mol Graphics* **1996**, *14*, 33−38.

(38) Wu, X.-L.; Sang, X.; Li, Z.; Tao, D. Study on physicochemical properties and basicity of carbanion-functionalized ionic liquids. *J. Mol. Liq.* **2020**, *312*, No. 113405.

(39) Moulder, J. F.; Stickle, W. F.; Sobol, W. M.; Bomben, K. D. *Handbook of X-Ray Photoelectron Spectroscopy.*; Perkin-Elmer, 1992.

(40) Rey, A.; Faraldos, M.; Casas, J. A.; Zazo, J. A.; Bahamonde, A.; Rodríguez, J. J. Catalytic wet peroxide oxidation of phenol over Fe/AC catalysts: Influence of iron precursor and activated carbon surface. *Appl. Catal., B* **2009**, *86*, 69−77.

(41) Wang, Y.; Hao, W.; Jacquemin, J.; Goodrich, P.; Atilhan, M.; Khraisheh, M.; Rooney, D.; Thompson, J. Enhancing Liquid-Phase Olefin−Paraffin Separations Using Novel Silver-Based Ionic Liquids. *J. Chem. Eng. Data* **2015**, *60*, 28−36.

(42) Abdel-Kader, N. S.; Abdel-Latif, S. A.; El-Ansary, A. L.; Sayed, A. G. Spectroscopic studies, density functional theory calculations, non-linear optical properties, biological activity of 1-hydroxy-4-((4-(N-(pyrimidin-2-yl)sulfamoyl)phenyl)diazenyl)-2-naphthoic acid and its chelates with Nickel (II), Copper (II), Zinc (II) and Palladium (II) metal ions. *J. Mol. Struct.* **2021**, *1223*, No. 129203.

(43) Li, H.; Zhang, Z.; Sun, G.; Liu, S.; An, L.; Li, X.; Li, H.; Gao, X. Performance and mechanism of the separation of C8 α-olefin from F-T synthesis products using novel Ag-DES. *AIChE J.* **2021**, *67*, No. e17252.

(44) Lu, T.; Chen, Q. Independent gradient model based on Hirshfeld partition: A new method for visual study of interactions in chemical systems. *J. Comput. Chem.* **2022**, *43*, 539−555.

(45) Bader, R. F. W. Atoms in molecules. *Acc. Chem. Res.* **1985**, *18*, 9−15.

(46) Lipkowski, P.; Grabowski, S. J.; Robinson, T. L.; Leszczynski, J. Properties of the C-H···H Dihydrogen Bond: An ab Initio and Topological Analysis. *J. Phys. Chem. A* **2004**, *108*, 10865−10872.

https://doi.org/10.1021/acsomega.5c00224
ACS Omega 2025, 10, 17744−17757